Molecular Therapy
Oncolytics
Original Article

Antitumor Activity *In Vivo* and *Vitro* of New Chiral Derivatives of Baicalin and Induced Apoptosis via the PI3K/Akt Signaling Pathway

Yi Hou,[1,4] Chao Pi,[1,4] Xianhu Feng,[1] Yuanyuan Wang,[1] Shaozhi Fu,[2] Xiaomei Zhang,[3] Ling Zhao,[1] and Yumeng Wei[1]

[1]Department of Pharmaceutics, School of Pharmacy, Southwest Medical University, No. 3-5, Zhongshan Road, Jiangyang District, Luzhou, Sichuan 646000, P.R. China; [2]Department of Oncology, The Affiliated Hospital of Southwest Medical University, No. 25, Taiping Street, Luzhou, Sichuan 646000, P.R. China; [3]Institute of Chinese Medicine and Pharmaceutical Chemistry, Chongqing Academy of Chinese Materia Medica, No. 34, Nanshan Road, Nanshan Street, Nan'an District, Chongqing 400065, P.R. China

In this study, a pair of chiral baicalin (BA) derivatives were synthesized by combining BA with phenylalanine methyl ester based on molecular docking technology, namely BAD and BAL. Cell cytotoxicity trails showed that the cell growth inhibitory effects of both BAD and BAL were increased by 8- to 12-fold compared with BA on A549 cells. Flow cytometry showed that the apoptotic rates of 50 μg/mL BA, BAD, and BAL to A549 cells for 48 h were 17.94%, 24.32%, and 39.69%, respectively. Western blotting analysis showed that BAD and BAL could promote Bax, caspase-3, and caspase-9 expression and inhibit Bcl-2 expression by inhibiting the expression of p-Akt. The tumor inhibition rates of BA, BAD, and BAL in nude mice of tumor-bearing experiment lasting for 24 days were 35.01%, 53.30%, and 59.35%, respectively. These results *in vitro* and *in vivo* showed that BAL had higher antitumor activity than did BAD and BA, which were related to promotion of the apoptosis of tumor cells by inhibiting the expression of p-Akt on PI3K/Akt pathway. This study provides an experimental basis for the development of a new configuration of BA for the treatment of cancer.

INTRODUCTION

Cancer has become one of the biggest threats to human health, and its incidence is increasing year by year. According to the World Health Organization (WHO) report in 2018, 18.1 million new cancer cases and more than 9.6 million deaths were reported worldwide. The top rankings were lung cancer and breast cancer at 11.6%, closely followed by colon cancer (10.2%) and prostate cancer (7.1%).[1–3] During the treatment of tumors, chemotherapy plays an irreplaceable role in the treatment and prognosis of tumors.[4,5] Unfortunately, the current efficacy of chemotherapy drugs is not ideal, and the tumor recurrence rate is high so that the 5-year survival rate is still low.[6,7] Therefore, it is necessary to develop more effective antitumor drugs.[8]

In recent years, researchers have tried to discover ingredients with potential antitumor activity from traditional Chinese medicines that have been used in clinic.[9,10] Li et al.[11] found that Xiaochaihu decoction, a traditional Chinese medicine prescription, could inhibit the growth of Eca-109 cells. Further research showed that baicalin (BA), a flavonoid extracted from *Scutellaria baicalensis* Georgi, as a main active monomer in Xiaochaihu decoction, could effectively inhibit the growth of tumor cells. Therefore, BA was considered as a potential antitumor natural active ingredient.[12–15] Among the antitumor mechanisms of BA, the phosphatidylinositol 3-kinase (PI3K)/Akt (also known as protein kinase B [PKB]) signal transduction pathway, considered as a primary pathway for tumor survival, is one of the important cell survival pathways *in vivo*.[16,17] Akt is the key node of PI3K/Akt. Blocking the phosphorylation process of Akt was considered to be one of the most of effective ways to promote tumor cell apoptosis.[18–21] Some studies have proved that BA could be used as a blocker of the Akt pathway to induce apoptosis of tumor cells.[22,23] For example, Xu et al.[24] found that BA could inhibit the proliferation and migration of A549 and DDP (cisplatin)-resistant A549 by inhibiting the overexpression of phosphorylated (p-)Akt. However, the relatively low antitumor activity of BA is the main factor restricting its application as a new antitumor drug. It is necessary to obtain the derivatives with high antitumor activity by structure modification of BA.

Many studies showed that phenylalanine (Phe) methyl ester (PME) with chiral structure can be used as an intermediate ligand to enhance the antitumor activity of drugs. Since the types and amounts of information transfer factors in tumor cells are different from normal cells, chiral drugs with spatial specificity have higher antitumor activity than do traditional chemotherapy drugs.[25–27] Phe, the origin of

Received 11 May 2020; accepted 27 August 2020;
https://doi.org/10.1016/j.omto.2020.08.018.

[4]These authors contributed equally to this work.

Correspondence: Ling Zhao, Department of Pharmaceutics, School of Pharmacy, Southwest Medical University, No. 3-5, Zhongshan Road, Jiangyang District, Luzhou, Sichuan 646000, P.R. China.
E-mail: zhaoling-998@163.com
Correspondence: Yumeng Wei, Department of Pharmaceutics, School of Pharmacy, Southwest Medical University, No. 3-5, Zhongshan Road, Jiangyang District, Luzhou, Sichuan 646000, P.R. China.
E-mail: weiyumeng-268@163.com

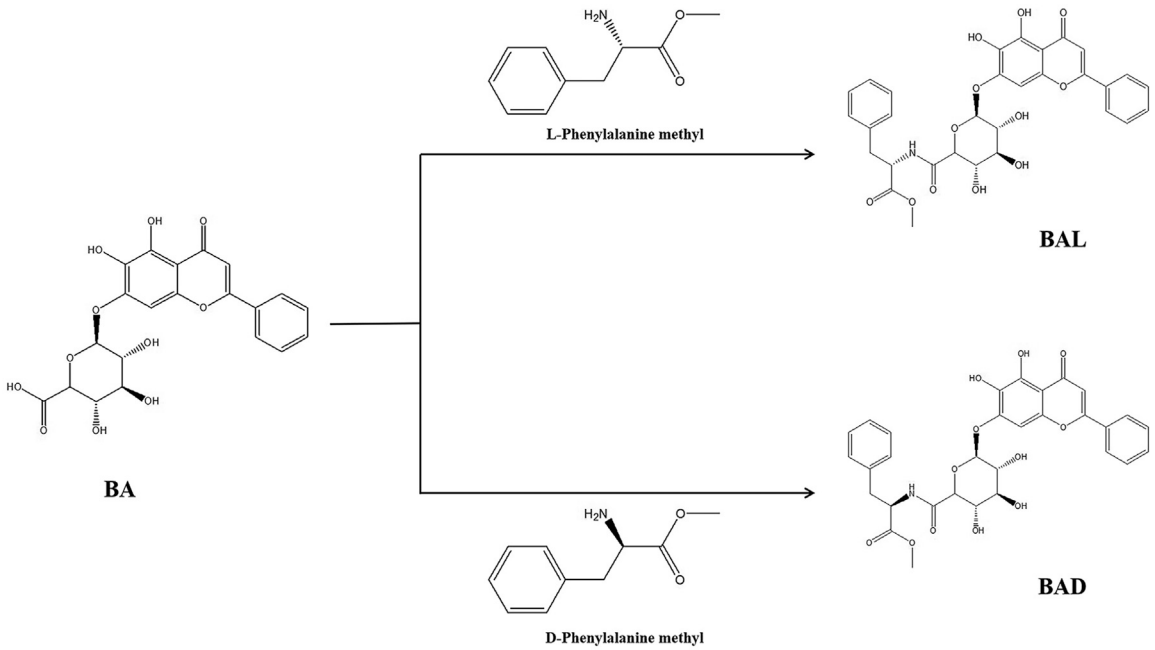

Figure 1. The Synthetic Route of BAD and BAL

PME, is one of the essential amino acids for human beings.[28,29] It has been found that Phe needed for the growth of cancer cells is 3- to 5-fold as much as that of normal cells. Clinical data showed that antineoplastic drugs such as the Phe nitrogen mustard, a derivative of Phe, have much higher antineoplastic activity and safety than do their parent drugs.[30] Meanwhile, Salehi et al.[31] found that a novel iron-chelating agent prepared with PME as a ligand could induce the apoptosis of tumor cells. Seiler et al.[32] found that the combination of proanthocyanidins and PME increased the apoptotic effect of proanthocyanidins on tumor cells. These data showed that PME can be used as an intermediate carrier of new anti-cancer compounds.

In this study, in order to overcome the defects of BA, a group of chiral derivatives of BA were designed and synthesized by PME to improve the antitumor activity of BA at the first time. Molecular docking technology showed that BAD and BAL can combine with Akt better than BA, and the antitumor activity *in vivo* and *vitro* and the apoptosis mechanism were studied.[33] We hope to provide an experimental basis for the development of BA derivatives and broaden the research and development of new antitumor drugs.

RESULTS

Characterization of BAD and BAL

BAD was characterized as follows: ^{1}H-nuclear magnetic resonance (NMR) (400 MHz, DMSO) chemical shift value (δ) 8.18 (singlet [s], ^{1}H), 8.14 (doublet [d], coupling constant [J] = 7.1 Hz, ^{1}H), 7.65–7.55 (multiplet [m], ^{2}H), 7.28 (triplet [t], J = 7.2 Hz, ^{2}H), 7.24–7.20 (m, ^{1}H), 7.20–7.15 (m, ^{4}H), 7.07 (doublet of doublets [dd], J = 10.0, 4.7 Hz, ^{2}H), 5.05 (d, J = 7.6 Hz, ^{1}H), 4.55 (dd, J = 14.0, 7.3 Hz, ^{1}H), 4.05 (d, J = 9.7 Hz, ^{1}H), 3.65 (dd, J = 13.4, 6.7 Hz, ^{3}H), 3.53–3.46 (m, ^{3}H), 3.44 (d, J = 9.1 Hz, ^{1}H), 3.39–3.31 (m, ^{2}H), 3.03 (d, J = 7.6 Hz, ^{1}H), 1.19 (d, J = 31.7 Hz, ^{3}H). Electrospray ionization mass spectrometry (ESI-MS) *m/z*; 606.40 metal hydride $[M-H]^{-}$.

BAL was characterized as follows: ^{1}H NMR (400 MHz, DMSO) δ 8.18 (s, ^{1}H), 8.14 (d, J = 7.0 Hz, ^{1}H), 7.64–7.52 (m, ^{2}H), 7.29 (t, J = 7.2 Hz, ^{2}H), 7.22 (t, J = 7.3 Hz, ^{1}H), 7.21–7.11 (m, ^{4}H), 7.07 (s, ^{1}H), 6.91 (t, J = 7.3 Hz, ^{1}H), 6.84 (t, J = 7.3 Hz, ^{1}H), 5.02 (d, J = 7.2 Hz, ^{1}H), 4.52 (td, J = 8.6, 5.0 Hz, ^{1}H), 4.04 (d, J = 9.7 Hz, ^{1}H), 3.79–3.67 (m, ^{1}H), 3.59 (s, ^{3}H), 3.55–3.48 (m, 1H), 3.45–3.30 (m, ^{2}H), 3.03 (dd, J = 13.6, 4.8 Hz, ^{1}H), 2.93–2.87 (m, ^{1}H), 1.20 (d, J = 28.7 Hz, ^{3}H). ESI-MS *m/z*; 606.40 $[M-H]^{-}$.

For the structures of BAD and BAL, see Figure 1.

Effect of BAD and BAL on Proliferation Inhibition of Tumor Cells

In an MTT (3-(4,5-dimethylthiazol-2-yl)-2,5-diphenyltetrazolium bromide) assay, lung cancer or breast cancer cells were treated with different concentrations of BAD and BAL (10, 20, 30, 40, 50 μg/mL) for 48 or 24 h, respectively. The results are shown in Figures 2 and 3. BAD and BAL had a stronger inhibitory effect on A549 cells than did BA ($p < 0.05$), and BAL is more sensitive than BAD (Figures 2A and 2B). The inhibition rates of 50 μg/mL BA, BAD, and BAL on A549 cells at 48 h were 31.07%, 88.95%, and 94.13%, respectively. These data suggested that the antitumor activity of A549 cells is BAL > BAD > BA ($p < 0.05$). For H460 cells (Figure 2C), The inhibition rate of BA of all concentrations at 24 h was less than 10%.

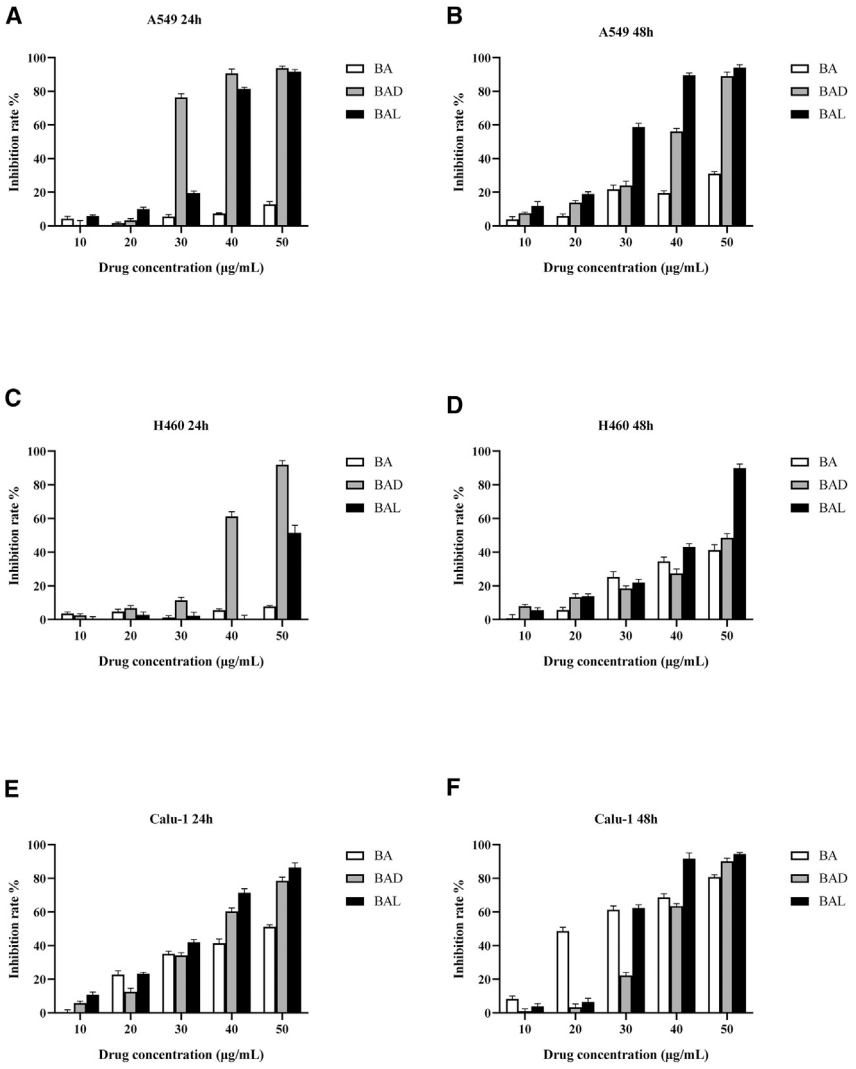

Figure 2. Inhibition Effects of BA, BAD, and BAL on the Growth of A549, H460, and Calu-1 Cell Lines for 24- and 48-h Treatments

The results are representative of at least three independent experiments run in triplicate. Data are expressed as means ± SD ($p < 0.05$, n = 5). (A and B) A549 cells, (C and D) H460 cells, (E and F) Calu-1 cells. (A, C, and E) 24-h treatment, (B, D, and F) 48-h treatment.

In breast cancer cell lines, BAD and BAL had little inhibitory effect on MBA-MB-435 at 24 and 48 h (Figures 3A and 3B). The inhibition rates of BAD and BAL for MBA-MB-435 cells were less than 25% at all concentrations, while BA showed good inhibitory activity and obvious concentration dependence. This result suggested that the cell line was sensitive to BA only. For MCF-7 cells (Figures 3C and 3D), when the concentration of drug was below 30 μg/mL, the three drugs were not sensitive to MCF-7 cells at 24 h. However, the inhibition rates of 50 μg/mL BAD and BAL were 62.56% and 60.58% at 24 h, which were significantly higher than that of BA (the inhibition rate of 50 μg/mL was 35.64%) ($p < 0.05$). Compared with 24 h, BA, BAD, and BAL showed stronger inhibitory effect on MCF-7 cells at 48 h, which was time-dependent. The sensitivity rates of BAD and BAL to T47D cells were significantly higher than that of BA ($p < 0.05$) at 24 h (Figure 3E). When the concentration of BAD and BAL increased to 30 μg/mL at 24 h, the inhibition rates of BAD and BAL for T47D cells were 71.18% and 82.32%, while the inhibition rate of BA for T47D cells at 50 μg/mL was only 31.30%. After 48 h, the sensitivity of BA was improved compared with 24 h, but its inhibition rate was still lower than those of BAD and BAL (Figure 3F).

However, when the concentration of BAD reached 40 μg/mL, the inhibitory effect of BAD on H460 cells increased rapidly to 61.32%, and the inhibitory effect of BAL at 50 μg/mL increased rapidly to 51.89%. Meanwhile, the inhibitory effect of each drug on H460 cells showed a concentration dependence at 48 h (Figure 2D). Interestingly, when the concentration of BAL reached 50 μg/mL at 48 h, the inhibitory rate of BAL for H460 cells was 89.94%. The inhibition rates of BA, BAD, and BAL on Calu-1 cells showed a good concentration-dependent relationship at 24 h (Figure 2E), but the inhibition effects of BAD and BAL were still stronger than that of BA at medium and high concentrations (>30 μg/mL). The inhibition rates of 50 μg/mL BA, BAD, and BAL on Calu-1 cells at 24 h were 51.15%, 78.46%, and 86.38%, respectively. As shown in Figure 2F, when the drug concentration was less than 30 μg/mL and the intervention time reached 48 h, the inhibitory effect of BA on Calu-1 cells was stronger than that of BAD and BAL ($p < 0.05$). However, BAD and BAL were slightly stronger than BA at high concentrations (>40 μg/mL).

The Apoptosis Effect of BAD and BAL in A549 Cells

Chan et al.[34] have proven that BA can induce apoptosis of cancer cells. In order to prove whether BAD and BAL can also induce apoptosis of A549 cells, with BA as the control, BAD and BAL were used to treat A549 cells at the dose of 50 μg/mL for 48 h. Flow cytometry showed that the apoptotic rates of BA, BAD, and BAL on A549 cells were 17.94%, 24.32%, and 39.69%, respectively (Figure 4H). The early apoptotic rates were 11.21%, 14.37%, and 34.41%, respectively, while the late apoptotic rates were 6.72%, 9.95%, and 5.27%, respectively. Staining results of Hoechst 33258 also showed that both BAD and BAL had a stronger effect on apoptosis of A549 cells than did BA, and BAL had the strongest effect (Figure 4A). However, the results of cell cycles showed that BA, BAD, and BAL were the same for A549 cells as the control group (Figures 4C–4E). It was suggested

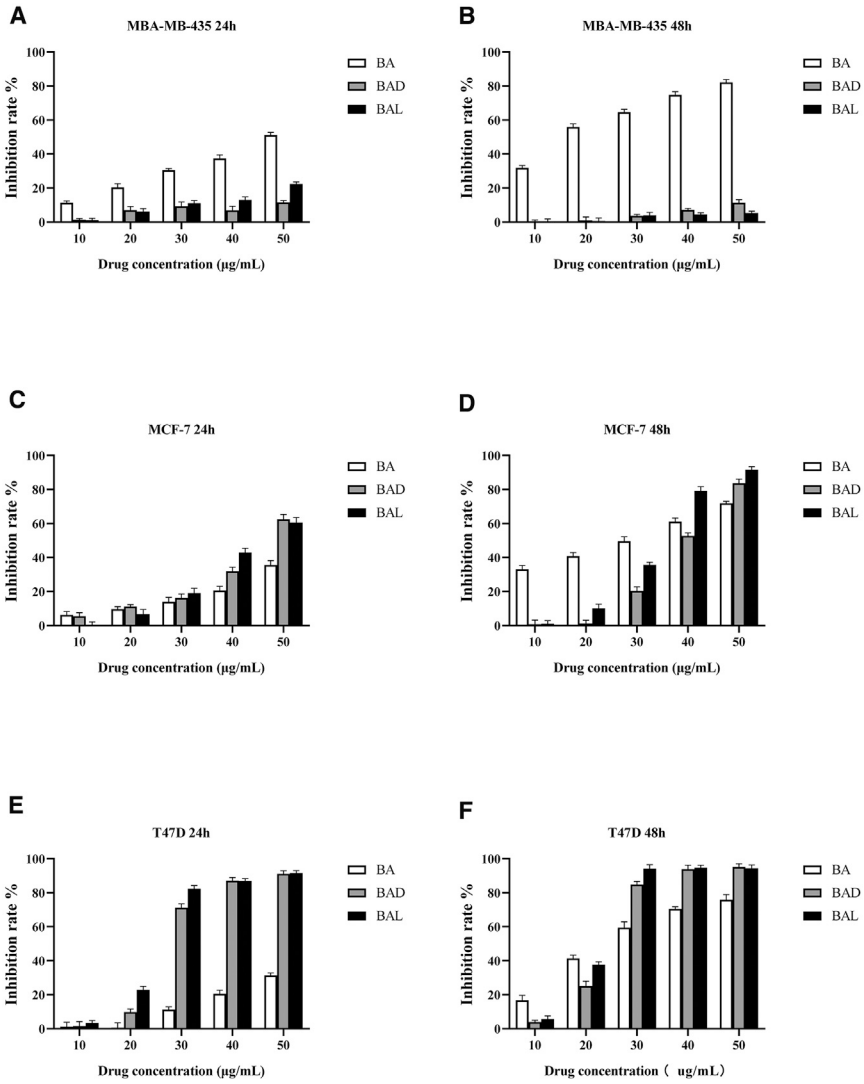

Figure 3. Inhibition Effects of BA, BAD, and BAL on the Growth of MBA-MB-435, MCF-7, and T47D Cell Lines for 24- and 48-h Treatments

The results are representative of at least three independent experiments run in triplicate. Data are expressed as means ± SD ($p < 0.05$, $n = 5$). (A and B) MBA-MB-435 cells, (C and D) MCF-7 cells, (E and F) T47D cells. (A, C, and E) 24-h treatment, (B, D, and F) 48-h treatment.

that the three drugs may not promote tumor cell death by interfering with cell cycle at this concentration.

These results suggested that both BAD and BAL can induce A549 cell apoptosis and ultimately inhibit cell proliferation. The induction effect of BAD and BAL is stronger than that of BA, which can inhibit the growth of A549 better. The results were consistent with those of MTT and were significantly different ($p < 0.001$).

The Mechanism of BAD and BAL Inducing Apoptosis

Many studies have shown that BA could inhibit the expression of p-Akt in the PI3K/Akt pathway to promote the apoptosis of tumor cells.[22–24] Molecular docking technology predicted that BAD and BAL could bind Akt protein better than BA, especially because BAL had the highest binding ability (total score >4) (Figure 5). To determine whether BAD or BAL promotes apoptosis the as same as BA by inhibiting the expression of p-Akt, western blot analysis was used to detect the expression of total Akt (T-Akt), p-Akt, Bax, Bcl-2, caspase-3, and caspase-9 proteins extracted from A549 cells with different concentrations of BA, BAD, and BAL. The results showed that BA, BAD, and BAL could inhibit the expression of p-Akt in a concentration-dependent trend (Figures 6A and 6B). The inhibitory effect of BAD and BAL on p-Akt was significantly stronger than BA. Interestingly, when the dose concentration was greater than 25 μg/mL, the effect of BAL on p-Akt was stronger than that of BAD ($p < 0.05$). The proportions of Bax/Bcl-2 in the three groups increased with the concentration and were significantly higher than that in the control group ($p < 0.01$) (Figure 6C). The effect of two chiral derivatives on Bax/Bcl-2 was greater than that on BA ($p < 0.05$). Caspase family proteins were the important components of cell apoptosis. As shown in Figures 6D–6F, the expression of caspase-9, the initiator of apoptosis, in the BAD and BAL groups was significantly higher than that in the BA group. Meanwhile, the relative expression of caspase-9 in the BAL group was higher than in the BAD group ($p < 0.05$). The expression of caspase-3, the executor of apoptosis in the three groups, was consistent with caspase-9. Meanwhile, the effect of BAL on caspase-9 and caspase-3 was higher than that of BAD ($p < 0.05$). All of the results showed that BAD and BAL could promote the apoptosis of A549 cells by affecting the expression of p-Akt in the PI3K/Akt pathway.

In Vivo Antitumor Study

All groups were orally administered a daily dose of 100 mg/kg for 24 days to investigate the inhibitory effects of BAD and BAL on tumors in nude mice. The weight of nude mice in each group decreased slightly before and after administration, but there was no significant difference between the administration group and the negative control group ($p > 0.05$). Compared with the blank group, BA, BAD, and BAL could inhibit the growth of tumors ($p < 0.01$). The inhibitory effects of BAD and BAL were stronger than that that of BA ($p < 0.05$). After 24 days of administration, the inhibition rates of BA, BAD, and BAL were 35.01%, 53.30%, and 59.35%, respectively (Figures 7D–7F).

24 days later, the nude mice were dissected and the tumors were removed. Hematoxylin and eosin (H&E) staining showed that the

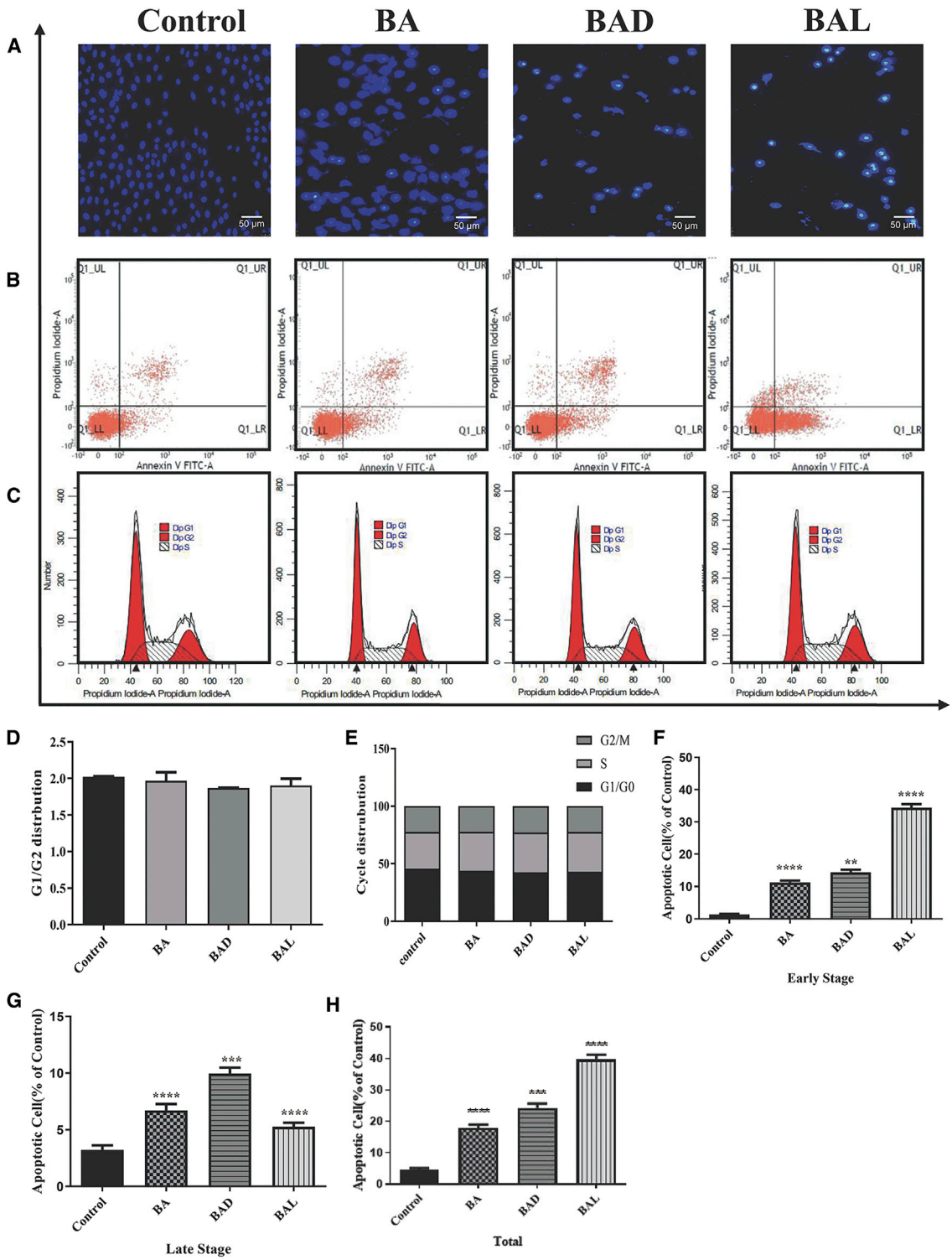

Figure 4. Results of Apoptosis and Cycle in A549 Cells

(A) The changes of nucleus of A549 cells stained by Hoechst 33258 with BA, BAD, and BAL of 50 μg/mL were observed under an inverted microscope. (B) Effects of BA, BAD, and BAL of 50 μg/mL on cell death were evidenced by annexin VFITC/PI double staining and FACS analysis. (C) Flow cytometry was performed to examine the effects of the cell cycle with BA, BAD, and BAL of 50 μg/mL in A549. (D) Ratio of G_1/G_2. (E) Frequency distribution bar chart for G_1/G_0, S, and G_2/M. (F) Early apoptosis of BAD and BAL to A549 cells at 48 h. (G) Late apoptosis of BAD and BAL to A549 cells at 48 h. (H) Total apoptosis of BAD and BAL to A549 cells at 48 h. *$p < 0.05$, **$p < 0.01$, ***$p < 0.001$, dose groups versus control.

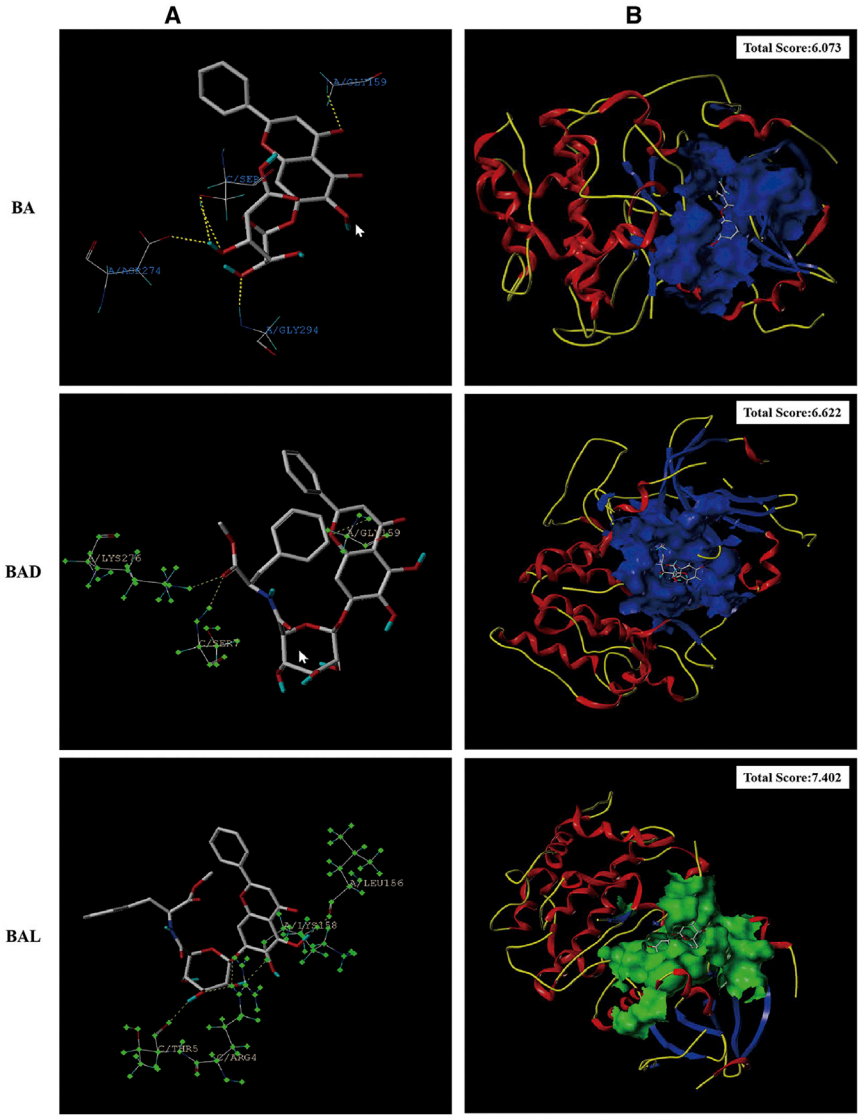

Figure 5. Results of Molecular Docking of Akt
(A) 3D interaction of BAD and BAL with amino acids. (B) 3D interaction of BAD and BAL with Akt protein.

growth of the tumors in the control group was vigorous and that the microvessels were abundant (Figure 7H). The degree of tumor necrosis induced by drugs was BAL > BAD > BA in the treatment group. Immunohistochemical results showed that the expression of CD31 in BAD and BAL were significantly decreased compared with that in the BA group (Figure 7G). These data further indicated that BAD and BAL could better inhibit tumor angiogenesis to inhibit tumor growth. Meanwhile, the inhibitory effect of BAL was better than that of BAD.

In agreement with the MTT results, these results demonstrate that BAD and BAL can inhibit the growth of tumors better in nude mice.

DISCUSSION

Chiral drugs refer to a group of isomers that are mirror images of each other by introducing chiral centers into drug molecules.[35–37] Most of the receptors and enzymes in organisms have chiral properties in their spatial structure. The affinity of the chiral drugs to their receptors is different due to the mirror symmetry of space arrangement, which leads to the difference of pharmacological activity, even the opposite pharmacological activity. Currently, most of the new anti-cancer drugs inhibit the growth of tumors by affecting the activity of key enzymes in a signaling pathway. Based on the specificity of enzyme space structure by molecular docking technology, discovering chiral drugs with high antitumor activity has become one of the hotpots of new drugs in recent years.[38–40] BAD and BAL are types of chiral drugs designed and synthesized based on molecular docking technology, which could improve the antitumor activity more than that for BA.

Lung cancer is one of the most common malignant tumors and an important cause of cancer death. According to statistics, in 2018, there were 2.1 million new cases of lung cancer worldwide and nearly 1.8 million deaths were caused directly or indirectly by lung cancer, accounting for 18.4% of cancer deaths.[1–3] Most lung cancers are found in the middle and late stages, and radical resection is difficult to achieve in surgical treatment.[41–43] In view of this, chemotherapy still plays an important role in the treatment of tumors. However, the relatively low efficiency, relatively high toxicity, high recurrence rate of lung cancer, and the appearance of drug resistance limited the use of chemotherapy drugs in the clinic. The development of new chemotherapeutic drugs with high antitumor activity has become a research hotspot in recent years.

BAD and BAL were screened to investigate their antitumor activity in lung cancer and breast cancer cell lines by an MTT assay. In breast cancer cell lines, the antitumor activity of BAD and BAL at T47D were significantly stronger than that of BA (Figures 3E and 3F). For MCF-7 cell lines, BAD and BAL showed high antitumor activity only at high concentrations (>40 μg/mL); when the concentration was lower than 40 μg/mL, the inhibitory effects of BAD and BAL on MCF-7 cells were lower than that of BA. This indicating that the antitumor activity of BAD and BAL on MCF-7 cells was not significantly increased at low concentrations (<40 μg/mL) (Figures 3C and 3D). In addition, BAD and BAL did not inhibit the

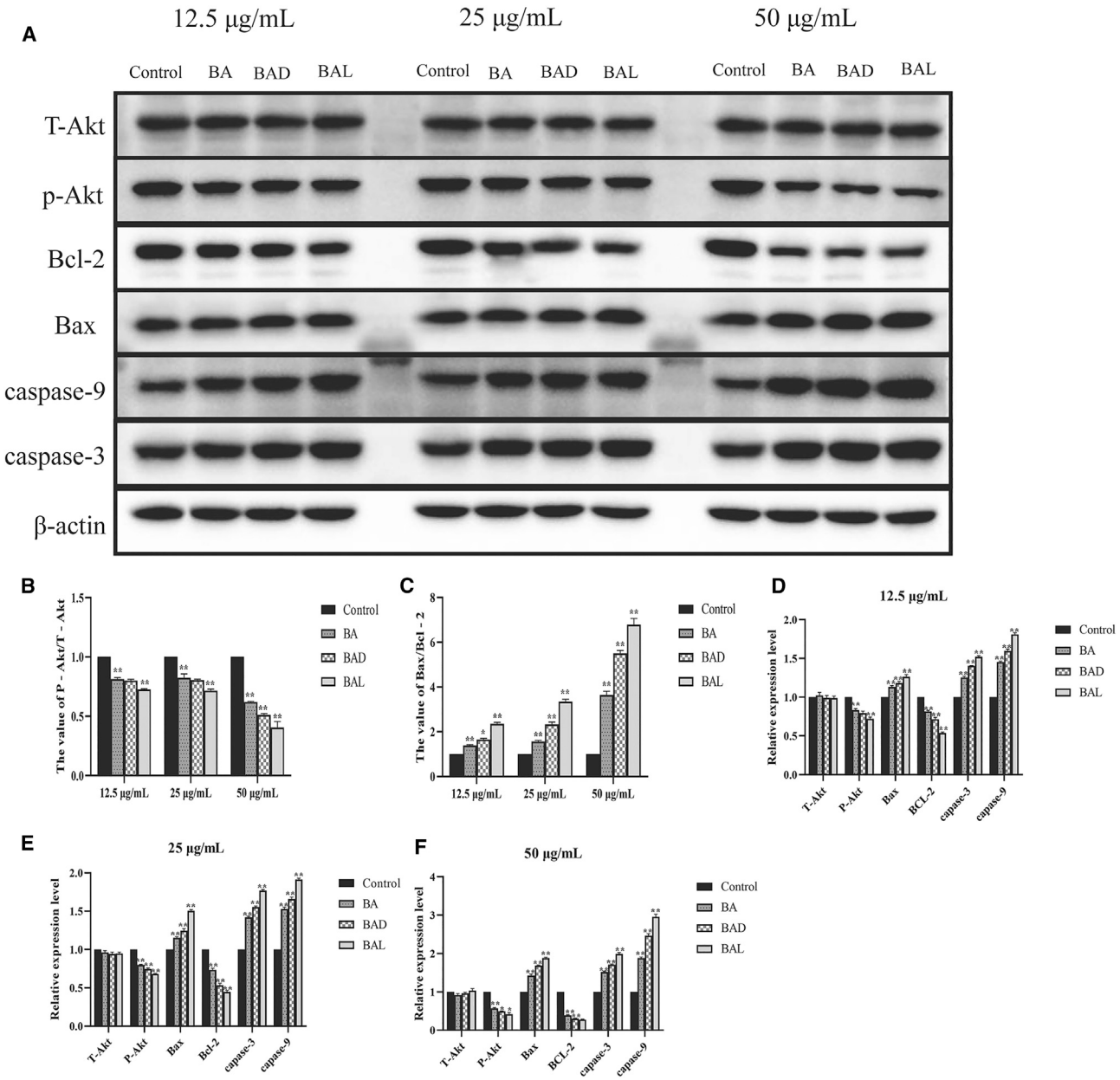

Figure 6. Results of Western Blotting

(A) Effects of BA, BAD, and BAL on the expression of T-Akt, p-Akt, Bax, Bcl-2, caspase-9, and caspase-3 by western blotting analysis at three concentrations in A549 cells for 48 h. (B) Effects of BA, BAD, and BAL on the value of p-Akt/T-Akt in A549 cells for 48 h. (C) Effects of BA, BAD, and BAL on the value of Bax/Bcl-2 in A549 cells for 48 h. (D) Effects of 12.5 μg/mL BA, BAD, and BAL on the expression of T-Akt, p-Akt, Bax, Bcl-2, caspase-9, and caspase-3 in A549 cells for 48 h. (E) Effects of 25 μg/mL BA, BAD, and BAL on the expression of T-Akt, p-Akt, Bax, Bcl-2, caspase-9, and caspase-3 in A549 cells for 48 h. (F) Effects of 50 μg/mL BA, BAD, and BAL on the expression of T-Akt, p-Akt, Bax, Bcl-2, caspase-9, and caspase-3 in A549 cells for 48 h. *$p < 0.05$, **$p < 0.01$, ***$p < 0.001$, dose groups versus control.

proliferation of MDA-MB-435 cells (Figures 3A and 3B); in contrast, BA showed higher antitumor activity. In lung cancer cell lines, BAD and BAL showed strong antitumor activity against lung cancer A549 cell lines compared with the BA group. The anti-cancer activity of BAL was more remarkable than that of BAD (Figures 2A and 2B). Yeom et al.[44] found that D-forms of chiral drugs or excipients can better enter tumor cells. BAD may lead to a higher inhibition rate than BAL to the A549 cell line at 24 h due to its better access to tumor cells. However, the inhibition rate of BAL was higher than that of BAD when the amount of BAD and BAL entering tumor cells was enough. For H460 cells, BAD and BAL exhibit high antitumor activity compared with BA at high concentrations (>40 μg/mL) (Figures 2C

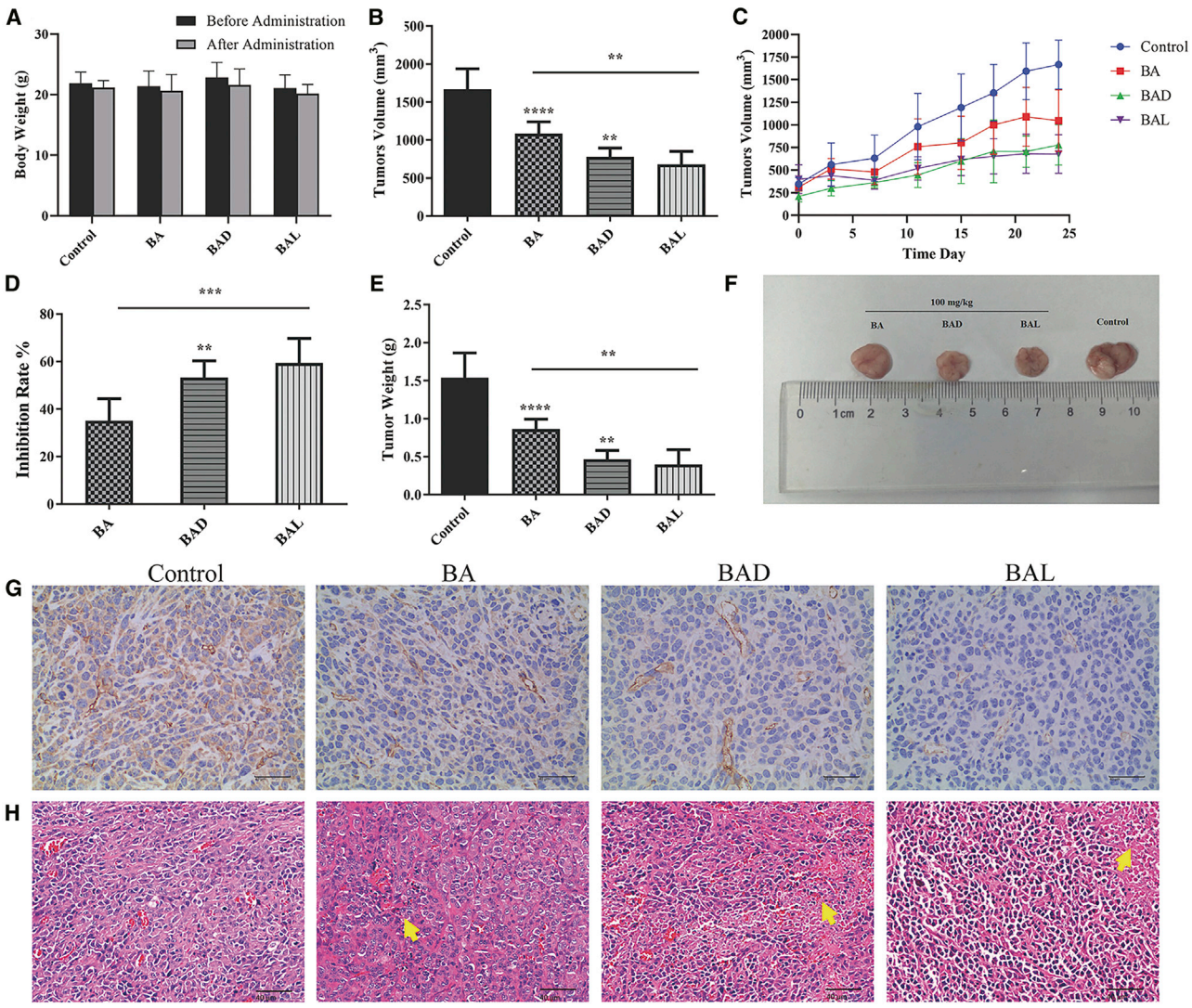

Figure 7. Antitumor Efficacy and Toxicity of BA, BAD, and BAL in Nude Mice Bearing A549 Tumor Xenografts *In Vivo*

(A) Changes of body weight (g) before and after treatment with BA, BAD, and BAL in nude mice. (B) Tumor volume of A549-bearing nude mice treated with BA, BAD, and BAL on day 24. (C) Changes of tumor volume with different groups in nude mice. (D) Tumor inhibitory rates (%) of A549-bearing nude mice treated with BA, BAD and BAL on day 24. (E) Tumor weights (g) of A549-bearing nude mice treated with BA, BAD, and BAL on day 24, after which the mice were humanely sacrificed. (F) Photograph of tumor on day 24 when the mice were humanely sacrificed. (G) The results of CD31 in tumor tissues were analyzed by immunohistochemistry. (H) The results of tumor mass H&E staining; the yellow arrow points to the necrotic tumor cells (means ± SD, n = 5). t test: *$p < 0.05$, **$p < 0.01$, ***$p < 0.001$, dose groups versus control.

and 2D). Interestingly, the inhibition rate of BAD at 48 h was lower than that at 24 h, which may be due to the high consumption of BAD and the proliferation of surviving H460 cells. For Calu-1 cells, the antitumor activity of BAD and BAL is still higher than that of BA in 24 h. However, when the drug action time of BAD and BAL reached 48 h, and the concentration was only above 40 μg/mL, their antitumor activity was higher than that of BA. Meanwhile, BA, BAD, and BAL inhibited the growth of Calu-1 cells in a concentration-dependent manner (Figures 2E and 2F). These results indicated that BAD and BAL with structural modification exhibit different anti-neoplastic activities for different cell lines due to the change of space structure. It was suggested that the space configuration of drugs plays an important role in their efficacy and targeting. Meanwhile, BAD and BAL showed high antitumor activity on lung cancer cells, especially in the A549 cell line with the high selectivity of BAL. These studies suggested that BAD and BAL are types of antitumor molecules with high clinical therapeutic value for lung cancer treatment.

Apoptosis plays an important role in the proliferation, drug resistance, and metastasis of tumors. BA has been shown to promote apoptosis of cancer cells through multiple pathways.[22,23,34] Our study showed that BAD and BAL can promote the apoptosis of tumors

more effectively than does BA. In particular, BAL mainly induced early apoptosis of A549 cells, and BAD mainly induced late apoptosis of A549 cells (Figure 4), which may be related to the difference in the spatial structure of BAD and BAL so as to result in a different ability of the trigger signal factor; more accurately, these findings may be due to the difference in the affinity of BAD and BAL to the receptor factor. Recent studies have shown that the spatial structure of drugs leads to an influence on cell apoptosis. The PI3K/Akt pathway is an intracellular signal transduction pathway with enzymatic activity, which regulates the proliferation and survival of cancer cells. Abnormal activity of the PI3K/Akt pathway not only leads to malignant transformation of cancer cells, but it also is related to the migration, adhesion, angiogenesis, and degradation of the extracellular matrix. Akt, as the core of this pathway, regulates the expression of target genes by phosphorylating downstream substrates.[18–21] Studies have shown that chiral substances with lactam structure can promote apoptosis of cancer cells by inhibiting the phosphorylation of Akt in the PI3K/Akt pathway, then upregulating caspase-3, caspase-9, and Bax, and downregulating the expression of Bcl-2 protein.[45] BAD and BAL are formed by BA and two PMEs through an amide bond; meanwhile, molecular docking technology predicts that BAD and BAL can better combine with Akt than can BA. Western blot analysis was used to explore the effect of BAD and BAL on the PI3K/Akt pathway. The results showed that BAD and BAL could inhibit the expression of p-Akt, and BAL was stronger than BAD (Figure 6). These effects also directly affected the downstream apoptotic proteins. The ratio of Bax/Bcl-2 regulated by p-Akt is the key factor to determine cell apoptosis, and these data indicated that the ratios of Bax/Bcl-2 in BAD and BAL were higher than in BA. Interestingly, the effects of BAD and BAL on caspase-9 and caspase-3 were the same as the ratio of Bax/Bcl-2. This suggested that BAD and BAL could promote the apoptosis of A549 cells by inhibiting the expression of p-Akt, and the selectivity of BAL was stronger than that of BAD.

Subsequently, an animal model with xenograft nude mice bearing A549 cells was established to further investigate the antitumor activity of BAD and BAL *in vivo*. At the end of the experiment, there was no death in each group, and there was no significant difference in the weight of each group compared with the control group (Figure 7A). The tumor volume of nude mice in the control group increased with time (Figure 7C). H&E staining showed that A549 cells grew actively and microvessels were abundant (Figure 7H). However, the tumor volume of nude mice in the experimental group decreased significantly. In particular, the BAL and BAD groups were both smaller than the BA group. H&E staining showed that all of the tumor cells in the three experimental groups showed necrosis. The results of immunohistochemistry also suggested that BAD and BAL could inhibit tumor angiogenesis better than BA (Figure 7G), and the effect was shown with BAL > BAD > BA (Figure 7H). The results of the experiment in nude mice once again proved that BAD and BAL had a strong inhibitory effect on tumors (Figures 7B–7F). The pharmacodynamics *in vivo* were consistent with the results of cytotoxicity *in vitro*. It has been proven that BAD and BAL, as chiral derivatives of BA, have higher anti-neoplastic activity than does BA in the treatment of lung cancer. BAD and BAL are potential anti-neoplastic drugs that are safe and effective in the treatment of lung cancer.

Conclusions

In conclusion, there were stronger tumor cell growth inhibition effects induced by BAD and BAL than that of BA, especially with high sensitivity to lung cancer. BAD and BAL had a good inhibitory effect on subcutaneous tumor growth *in vivo*, which was consistent with the results *in vitro*. The mechanism of that may induce the apoptosis of tumor cells by inhibiting the expression of p-Akt to promote Bax, caspase-3, caspase-9 expression and inhibit Bcl-2 expression.

MATERIALS AND METHODS

Materials and Instruments

BA (purity >98%), 1-hydroxybenzotriazole (purity >98%), and 1-ethyl-3-(3-dimethylaminopropyl)carbodiimide (EDCI) (purity >95%) were purchased from Best Company (Chengdu, China). Other reagents are analytical reagents, purchased from China Kelong. The structures of BAD and BAL are shown in Figure 1, which were confirmed by ^{1}H-NMR spectroscopy and liquid chromatography-mass spectrometry (LC-MS) analysis.

Synthesis of BAD and BAL

0.5 mmol of BA, 0.6 mmol of 1-hydroxybenzotriazole (HOBT), 0.9 mmol of 1-ethyl-(3-dimethylaminopropyl)carbonyl diimide hydrochloride (EDC.HCL) were dissolved in *N*,*N*-dimethylformamide (DMF), and reacted at room temperature for 6 h. Later, 1.5 mmol of L-Phe methyl ester hydrochloride (LBMS) or D-Phe methyl ester hydrochloride (DBMS) dissolved in DMF and triethylamine (TEA) were added, and the reaction lasted for 48 h at 50°C. The solvent of the mixture was removed by rotary evaporation, and the desire products were separated by column chromatography (silica gel, dichloromethane/methanol/formic acid = 19:1:0.5) and were purified by recrystallization with ethanol.

Cell Culture

Breast cancer MCF-7, MBA-MB-435, and T47D cells and lung cancer A549, H460, and Calu-1 cells were obtained from the Shanghai Cell Bank (China). All cells were cultured in a 5% CO_2 incubator (with a HEPA class 100 filter) in RPMI 1640 or DMEM medium of 100 U/mL of penicillin-streptomycin and 10% fetal bovine serum. Medium was replaced three times a week. Cells were used during the exponential growth phase of all experiments.

Cell Viability Assay

The drug mother liquor of 100 μg/mL was prepared in the medium containing 0.1% dimethyl sulfoxide (DMSO) as solvent. At the same time, the drug solution was diluted to 10, 20, 30, 40, and 50 μg/mL, respectively. Cells were inoculated into 96-well plates at a concentration of 2×10^4 cells/well. Next, the cells were treated with various concentrations of drug solutions in triplicate. 24 and 48 h later, 20 μL of MTT (5 mg/mL) was added to each pore and the cells were cultured in darkness at 37°C for 4 h. After removing

the equipartition samples, the remaining crystals (methyl sulfoxide precipitate) were dissolved with 150 μL of DMSO, the cells were cultured at 37°C for 10 min, and the absorbance (optical density [OD]) was measured with ELISA at 570 nm. Cell viability was determined by an MTT assay. The cell inhibition rate was calculated as follows: inhibition rate = $[(OD_{control} - OD_{treated})/OD_{control}] \times 100\%$.

Cell Apoptosis and Cycle

A549 cells were inoculated into six-well plates at a concentration of 4×10^5 cells/well. Cells were fixed with 4% paraformaldehyde for 15 min and washed twice with PBS. Subsequently, Hoechst 33258 was used for staining. Under ×200 magnification, the morphology of the nucleus was observed with a fluorescence microscope. The Hoechst 33258 kit was from the Beyotime Institute of Biotechnology.

A549 cells were inoculated into six-well plates. After adherence, BA, BAD, and BAL were used to interfere with A549 cells in logarithmic growth phase. The concentration gradients of A549 cells were 50 μg/mL. At the same time, the control group was set up without administration. After 48 h, the supernatant was removed, and the cells were digested and collected by trypsinase without EDTA. PBS was washed twice at 3,000 rpm. After centrifugation for 10 min, 1 mL of buffer suspension was added. First, 5 μL of annexin V/fluorescein isothiocyanate (FITC) was added, and then 5 μL of annexin V/propidium iodide (PI) was added. Oscillating and mixing were performed. Light-shielding staining was performed for 30 min. Finally, apoptosis rate was determined by flow cytometer (FACSCalibur, BD Biosciences, San Jose, CA, USA) and FlowJo software.

A549 cells were inoculated into six-well plates at a concentration of 4×10^5 cells/well. The cells were incubated with 50 μg/mL of BA, BAD, and BAL for 24 h. All cells were digested with trypsin, washed twice with PBS, and then fixed in PBS with 70% dry ice-ethanol for 30 min at −20°C. Finally, the cells were washed twice with PBS, dealing with RNase A (10 mg/mL), and then suspended in 50 μg/mL PI for dyeing. Flow cytometry (BD Biosciences, San Jose, CA, USA) was used for cell cycle distribution.

Western Blot Analysis

SYBYL-X 2.0 software was used to verify the affinity of derivatives to amino acids and proteins. A total score of >4 was considered as high affinity. Western blot was used to detect the expression levels of T-Akt, p-Akt, Bax, Bcl-2, caspase-3, and caspase-9. Three concentrations (50, 25, and 12.5 μg/mL) of BA, BAD, and BAL were used to treat A549 cells for 48 h. The control group was given the culture medium without drugs. The cell protein was collected and lysed by lysate. Protein content was determined by the phenylmethanesulfonylfluoride (PMSF) method. The protein was separated by SDS-PAGE and then transferred to a nitrocellulose (NC) membrane. The NC membrane was non-specific binding blocked by 5% milk for 1 h in TBST (5 mM Tris-HCl, 136 mM NaCl, 0.05% Tween 20 [pH 7.6]). The membranes were cultured with primary antibodies of Akt (1:1,000), p-Akt (1:1,000), Bax (1:5,000), Bcl-2 (1:2,000), caspase-3 (1:2,000), caspase-9 (1:1,000), and β-actin (1:100,000) at 4°C overnight. The membranes were rinsed three times with 1× TBST and incubated with secondary antibodies (1:1,000) for 2 h at room temperature. Finally, the membranes were washed three times with 1× TBST. Protein bands were visualized by an ECL (enhanced chemiluminescence) system (Amersham Biosciences, USA). The gray values of T-Akt, p-Akt, Bax, Bcl-2, caspase-3, and caspase-9 proteins were measured by Quantity One software.

Nude Mice

Twenty-four nude mice (12 males and 12 females) aged 4 weeks and weighing 18–22 g were purchased from Chengdu Dashuo Biotechnology (Chengdu, China, license no. SCXK [Chuan] 2013-24). According to the national requirements for animal welfare, all nude mice were in the VIC Animal Breeding Room of the Animal Breeding Center of Southwest Medical University. The room temperature was 18°C–22°C and the relative humidity was 40%–70%. The nude mice were provided with sufficient food and pure water. All the in vivo experimental protocols were approved by the animal care committee of Southwest Medical University.

Nude Mice Xenograft Models

A549 cells in the logarithmic phase of growth were collected for inoculation. Nude mice were injected with A549 cells (1×10^7 cells/mL) in 0.1 mL of PBS in the right hip. Two vertical diameters were measured daily with a digital caliper to monitor the size of xenografts. After 7 days, the maximum diameter of the tumors was between 5 and 7 mm. Twenty-four nude mice were randomly divided into four groups: (1) saline control group, (2) 100 mg/kg BA group, (3) 100 mg/kg BAD group, and (4) 100 mg/kg BAL group. Each mouse in the experimental group was orally administered BA, BAD, or BAL once a day for 24 days. The weight of every mouse was measured once a day.

Tumor Volume and Weight

The tumor volume was measured with a Vernier caliper, and the weight of nude mice in each group was measured every 3 days. The formula $V = \pi/6(ab^2)$ was chosen to calculate the volume (V) of tumors, where a and b represent the largest and shortest vertical axes, respectively. After 24 days of administration, nude mice were sacrificed by cervical dislocation and autopsy was performed. All xenografts of tumors were isolated from nude mice and analyzed. The weight of tumors was measured. The tumor inhibition rate (IR) was calculated as follows: $IR = (1 - \text{tumor weight}_{drug}/\text{tumor weight}_{control}) \times 100\%$. The weight and volume of each tumor were plotted and compared with those of the control group. Tumor tissue was fixed with formalin buffered by 10% phosphate, embedded in paraffin, stained with H&E, and observed under light microscope. All experimental procedures were performed in a blinded manner.

Immunohistochemistry

Tumor tissues were fixed in 4% paraformaldehyde for 24 h and dehydrated and embedded to prepare tumor sections. Antigen retrieval of tissue sections was performed for 3 min at 95°C in 0.01 M citric acid buffer (pH 6.0). Sections were incubated by the primary antibody

(1:100) of CD31 overnight at 4°C, and then incubated by the second antibody for 2 h at 37°C. Finally, after development with 3,3′- diaminobenzidine (DAB) and hematoxylin staining, immunohistochemical signals were imaged and observed under a microscope. Staining was assessed by bright-field light microscopy.

Statistical Analysis

Statistical data were summarized as mean ± standard deviation by SPSS 19.0 software. Univariate analysis of variance and a Tukey's test were used for inter-group comparison. A p value of <0.05 was considered statistically significant.

AUTHOR CONTRIBUTIONS

Y.H. and C.P. conducted the experiments and wrote the paper. X.F., Y.W., S.F., and X.Z. analyzed the data and revised the paper. Y.W. and L.Z. designed the experiments and directed the study. All authors read and approved the final manuscript.

CONFLICTS OF INTEREST

The authors declare no competing interests.

ACKNOWLEDGMENTS

This study was supported by the basic research fund of the Science and Technology Department of Sichuan Province of China (nos. 2020YJ0336 and 2020YJ0373), the Joint Fund of Luzhou City and Southwest Medical University (nos. 2017LZXNYD-T02 and 2019LZXNYDZ07), the Science and Technology Fund of Luzhou Science and Technology and Human Resources Bureau (no. 2019-SYF-35), the Science and Technology Innovation Team from Jiucheng Science and Technology Talent Cultivation Plan in Luzhou City (no. 2019-1), the Scientific Research Foundation of the Education Department of Sichuan Province (nos. 17ZA0439 and 18ZB0646), and by a research grant from the Traditional Chinese Medicine Administration in Sichuan Province (no. 2018QN069).

REFERENCES

1. Wasan, H.S., Gibbs, P., Sharma, N.K., Taieb, J., Heinemann, V., Ricke, J., Peeters, M., Findlay, M., Weaver, A., Mills, J., et al.; FOXFIRE Trial Investigators; SIRFLOX Trial Investigators; FOXFIRE-Global Trial Investigators (2017). First-line selective internal radiotherapy plus chemotherapy versus chemotherapy alone in patients with liver metastases from colorectal cancer (FOXFIRE, SIRFLOX, and FOXFIRE-Global): a combined analysis of three multicentre, randomised, phase 3 trials. Lancet Oncol. *18*, 1159–1171.
2. Bray, F., Ferlay, J., Soerjomataram, I., Siegel, R.L., Torre, L.A., and Jemal, A. (2018). Global cancer statistics 2018: GLOBOCAN estimates of incidence and mortality worldwide for 36 cancers in 185 countries. CA Cancer J. Clin. *68*, 394–424.
3. Brierley, J., O'Sullivan, B., Asamura, H., Byrd, D., Huang, S.H., Lee, A., Piñeros, M., Mason, M., Moraes, F.Y., Rösler, W., et al. (2019). Global Consultation on Cancer Staging: promoting consistent understanding and use. Nat. Rev. Clin. Oncol. *16*, 763–771.
4. Hellmann, M.D., Li, B.T., Chaft, J.E., and Kris, M.G. (2016). Chemotherapy remains an essential element of personalized care for persons with lung cancers. Ann. Oncol. *27*, 1829–1835.
5. Ahles, T.A., and Root, J.C. (2018). Cognitive effects of cancer and cancer treatments. Annu. Rev. Clin. Psychol. *14*, 425–451.
6. Owens, D.K., Davidson, K.W., Krist, A.H., Barry, M.J., Cabana, M., Caughey, A.B., Doubeni, C.A., Epling, J.W., Jr., Kubik, M., Landefeld, C.S., et al.; US Preventive Services Task Force (2019). Medication use to reduce risk of breast cancer: US Preventive Services Task Force recommendation statement. JAMA *322*, 857–867.
7. Weingart, S.N., Zhang, L., Sweeney, M., and Hassett, M. (2018). Chemotherapy medication errors. Lancet Oncol. *19*, e191–e199.
8. Zhou, J., Yu, G., and Huang, F. (2017). Supramolecular chemotherapy based on host-guest molecular recognition: a novel strategy in the battle against cancer with a bright future. Chem. Soc. Rev. *46*, 7021–7053.
9. Zhao, L., Wei, Y., Huang, Y., He, B., Zhou, Y., and Fu, J. (2013). Nanoemulsion improves the oral bioavailability of baicalin in rats: in vitro and in vivo evaluation. Int. J. Nanomedicine *8*, 3769–3779.
10. Wei, Y., Guo, J., Zheng, X., Wu, J., Zhou, Y., Yu, Y., Ye, Y., Zhang, L., and Zhao, L. (2014). Preparation, pharmacokinetics and biodistribution of baicalin-loaded liposomes. Int. J. Nanomedicine *9*, 3623–3630.
11. Li, X., Sun, M., Zhao, Z., Yang, J., and Chen, K. (2014). Research on effect of minor bupleurum decoction of proliferation and apoptosis of esophageal cancer cell strain eca-109 cell. Pak. J. Pharm. Sci. *27* (5, Suppl), 1675–1679.
12. Jin, B.R., and An, H.J. (2020). Baicalin alleviates benign prostate hyperplasia through androgen-dependent apoptosis. Aging (Albany NY) *12*, 2142–2155.
13. Dong, L.H., Wen, J.K., Miao, S.B., Jia, Z., Hu, H.J., Sun, R.H., Wu, Y., and Han, M. (2010). Baicalin inhibits PDGF-BB-stimulated vascular smooth muscle cell proliferation through suppressing PDGFRβ-ERK signaling and increase in p27 accumulation and prevents injury-induced neointimal hyperplasia. Cell Res. *20*, 1252–1262.
14. Zhao, Q., Cui, M.Y., Levsh, O., Yang, D., Liu, J., Li, J., Hill, L., Yang, L., Hu, Y., Weng, J.K., et al. (2018). Two CYP82D enzymes function as flavone hydroxylases in the biosynthesis of root-specific 4′-deoxyflavones in *Scutellaria baicalensis*. Mol. Plant *11*, 135–148.
15. Ma, Z., Otsuyama, K., Liu, S., Abroun, S., Ishikawa, H., Tsuyama, N., Obata, M., Li, F.J., Zheng, X., Maki, Y., et al. (2005). Baicalein, a component of *Scutellaria radix* from Huang-Lian-Jie-Du-Tang (HLJDT), leads to suppression of proliferation and induction of apoptosis in human myeloma cells. Blood *105*, 3312–3318.
16. He, L., Liu, X., Yang, J., Li, W., Liu, S., Liu, X., Yang, Z., Ren, J., Wang, Y., Shan, L., et al. (2018). Imbalance of the reciprocally inhibitory loop between the ubiquitin-specific protease USP43 and EGFR/PI3K/AKT drives breast carcinogenesis. Cell Res. *28*, 934–951.
17. LoPiccolo, J., Blumenthal, G.M., Bernstein, W.B., and Dennis, P.A. (2008). Targeting the PI3K/Akt/mTOR pathway: effective combinations and clinical considerations. Drug Resist. Updat. *11*, 32–50.
18. Zhang, L., Li, Y., Wang, Q., Chen, Z., Li, X., Wu, Z., Hu, C., Liao, D., Zhang, W., and Chen, Z.S. (2020). The PI3K subunits, P110α and P110β are potential targets for overcoming P-gp and BCRP-mediated MDR in cancer. Mol. Cancer *19*, 10.
19. Verret, B., Cortes, J., Bachelot, T., Andre, F., and Arnedos, M. (2019). Efficacy of PI3K inhibitors in advanced breast cancer. Ann. Oncol. *30* (*Suppl 10*), x12–x20.
20. Ippen, F.M., Grosch, J.K., Subramanian, M., Kuter, B.M., Liederer, B.M., Plise, E.G., Mora, J.L., Nayyar, N., Schmidt, S.P., Giobbie-Hurder, A., et al. (2019). Targeting the PI3K/Akt/mTOR pathway with the pan-Akt inhibitor GDC-0068 in PIK3CA-mutant breast cancer brain metastases. Neuro-oncol. *21*, 1401–1411.
21. Mayer, I.A., and Arteaga, C.L. (2016). The PI3K/AKT pathway as a target for cancer treatment. Annu. Rev. Med. *67*, 11–28.
22. Huang, Y., Hu, J., Zheng, J., Li, J., Wei, T., Zheng, Z., and Chen, Y. (2012). Down-regulation of the PI3K/Akt signaling pathway and induction of apoptosis in CA46 Burkitt lymphoma cells by baicalin. J. Exp. Clin. Cancer Res. *31*, 48.
23. Zakki, S.A., Cui, Z.G., Sun, L., Feng, Q.W., Li, M.L., and Inadera, H. (2018). Baicalin augments hyperthermia-induced apoptosis in U937 cells and modulates the MAPK pathway via ROS generation. Cell. Physiol. Biochem. *45*, 2444–2460.
24. Xu, Z., Mei, J., and Tan, Y. (2017). Baicalin attenuates DDP (cisplatin) resistance in lung cancer by downregulating MARK2 and p-Akt. Int. J. Oncol. *50*, 93–100.
25. Lloyd, M.D., Yevglevskis, M., Lee, G.L., Wood, P.J., Threadgill, M.D., and Woodman, T.J. (2013). α-Methylacyl-CoA racemase (AMACR): metabolic enzyme, drug metabolizer and cancer marker P504S. Prog. Lipid Res. *52*, 220–230.
26. Zhou, Q., Yu, L.S., and Zeng, S. (2014). Stereoselectivity of chiral drug transport: a focus on enantiomer-transporter interaction. Drug Metab. Rev. *46*, 283–290.

27. Chu, S., Liu, S., Duan, W., Cheng, Y., Jiang, X., Zhu, C., Tang, K., Wang, R., Xu, L., Wang, X., et al. (2016). The anti-dementia drug candidate, (−)-clausenamide, improves memory impairment through its multi-target effect. Pharmacol. Ther. *162*, 179–187.

28. Singh, R.H., Rohr, F., Frazier, D., Cunningham, A., Mofidi, S., Ogata, B., Splett, P.L., Moseley, K., Huntington, K., Acosta, P.B., et al. (2014). Recommendations for the nutrition management of phenylalanine hydroxylase deficiency. Genet. Med. *16*, 121–131.

29. Cui, J.D., Qiu, J.Q., Fan, X.W., Jia, S.R., and Tan, Z.L. (2014). Biotechnological production and applications of microbial phenylalanine ammonia lyase: a recent review. Crit. Rev. Biotechnol. *34*, 258–268.

30. Paramo, J.C., Benavides, C., Tang, L.W., Martinez, A., Cabello-Inchausti, B., Davila, E., and Mesko, T.W. (2004). Complete remission of previously intractable peripheral cutaneous T-cell lymphoma of the lower extremity using isolated hyperthermic limb perfusion with melphalan (1-phenylalanine mustard). Cancer Invest. *22*, 545–549.

31. Salehi, S., Saljooghi, A.S.h., and Shiri, A. (2016). Synthesis, characterization and in vitro anticancer evaluations of two novel derivatives of deferasirox iron chelator. Eur. J. Pharmacol. *781*, 209–217.

32. Seiler, N., Chaabi, M., Roussi, S., Gossé, F., Lobstein, A., and Raul, F. (2006). Synergism between apple procyanidins and lysosomotropic drugs: potential in chemoprevention. Anticancer Res. *26* (5A), 3381–3385.

33. Zhao, L., Wei, Y., Pi, C., Huang, Y., Hou, Y., Feng, X., et al. (2019-12-24). Baicalin derivatives, their preparation and application. China CN201911342169.4[P]. (National Intellectual Property Administration).

34. Chan, F.L., Choi, H.L., Chen, Z.Y., Chan, P.S., and Huang, Y. (2000). Induction of apoptosis in prostate cancer cell lines by a flavonoid, baicalin. Cancer Lett. *160*, 219–228.

35. Gumustas, M., Ozkan, S.A., and Chankvetadze, B. (2018). Analytical and preparative scale separation of enantiomers of chiral drugs by chromatography and related methods. Curr. Med. Chem. *25*, 4152–4188.

36. Leek, H., Thunberg, L., Jonson, A.C., Öhlén, K., and Klarqvist, M. (2017). Strategy for large-scale isolation of enantiomers in drug discovery. Drug Discov. Today *22*, 133–139.

37. Sanganyado, E., Lu, Z., Fu, Q., Schlenk, D., and Gan, J. (2017). Chiral pharmaceuticals: a review on their environmental occurrence and fate processes. Water Res. *124*, 527–542.

38. Zhou, Y., Wu, S., Zhou, H., Huang, H., Zhao, J., Deng, Y., Wang, H., Yang, Y., Yang, J., and Luo, L. (2018). Chiral pharmaceuticals: environment sources, potential human health impacts, remediation technologies and future perspective. Environ. Int. *121*, 523–537.

39. Tibrewal, N., and Tang, Y. (2014). Biocatalysts for natural product biosynthesis. Annu. Rev. Chem. Biomol. Eng. *5*, 347–366.

40. Tao, J., and Xu, J.H. (2009). Biocatalysis in development of green pharmaceutical processes. Curr. Opin. Chem. Biol. *13*, 43–50.

41. Ho, J.C., and Leung, C.C. (2018). Management of co-existent tuberculosis and lung cancer. Lung Cancer *122*, 83–87.

42. Jacobsen, M.M., Silverstein, S.C., Quinn, M., Waterston, L.B., Thomas, C.A., Benneyan, J.C., and Han, P.K.J. (2017). Timeliness of access to lung cancer diagnosis and treatment: a scoping literature review. Lung Cancer *112*, 156–164.

43. Arbour, K.C., and Riely, G.J. (2019). Systemic therapy for locally advanced and metastatic non-small cell lung cancer: a review. JAMA *322*, 764–774.

44. Yeom, J., Guimaraes, P.P.G., Ahn, H.M., Jung, B.K., Hu, Q., McHugh, K., Mitchell, M.J., Yun, C.O., Langer, R., and Jaklenec, A. (2020). Chiral supraparticles for controllable nanomedicine. Adv. Mater. *32*, e1903878.

45. Hwang, S.J., Park, H.G., Park, Y., and Lee, H.J. (2016). An α-quaternary chiral latam derivative, YH-304 as a novel broad-spectrum anticancer agent. Int. J. Oncol. *49*, 2480–2486.